On the decay of a turbulent vortex ring

Alexander Weigand and Morteza Gharib

Citation: Phys. Fluids **6**, 3806 (1994); doi: 10.1063/1.868371
View online: http://dx.doi.org/10.1063/1.868371
View Table of Contents: http://pof.aip.org/resource/1/PHFLE6/v6/i12
Published by the AIP Publishing LLC.

On the decay of a turbulent vortex ring

Alexander Weigand and Morteza Gharib
California Institute of Technology, Graduate Aeronautical Laboratories, Pasadena, California 91125

(Received 9 May 1994; accepted 16 August 1994)

The spatiotemporal evolution of a turbulent vortex ring with an initial Reynolds number of 7500 is experimentally investigated using the technique of digital particle image velocimetry. The flow is initially characterized by the laminar/turbulent transition via azimuthal bending instabilities. After transition, the shedding of vorticity from peripheral regions of the ring is found to be responsible for the formation of a wake region. This shedding process results in the staircase-like decay of the circulation and propagation speed of the vortex ring. © *1994 American Institute of Physics.*

In a recent review article, Shariff and Leonard[1] describe turbulent vortex rings and puffs as one of the "least understood" turbulent shear flows. They classify three different types of turbulent vortex rings: those where turbulence initiates naturally at the nozzle of the generator; vortex rings that are initially laminar and undergo natural transition to turbulence by azimuthal bending instabilities; and turbulent puffs that are generated, for example, by placing a perforated plate at the nozzle exit. In contrast to previous investigations of Sallet and Widmayer,[2] Maxworthy,[3] and Glezer and Coles,[4] this Letter focuses on the evolution of vortex rings that are characterized by the natural transition from laminar to turbulent flow via azimuthal bending instabilities.

As Fig. 1 shows, vortex rings of diameter D, circulation Γ and propagation speed U_V are generated in a water tank by a piston-driven vortex-ring generator. The cylindrical nozzle has a diameter of $D_0=2.0$ cm, and its outer contour is wedge shaped with a tip angle of $\alpha=15°$. A linear microstepping motor controls the trapezoidal velocity profile of the piston with a stroke to nozzle-diameter ratio of $L_0/D_0=2.3$, an average piston velocity of $U_P=18.3$ cm/s, and an acceleration and deceleration of $|a|=3.05$ m/s^2. These initial conditions result in vortex rings with an initial Reynolds number of $\mathrm{Re}=\Gamma_0/\nu=7500$, where ν is the kinematic viscosity. The temporal origin $t=0$ corresponds to the initiation of the piston motion. The flow was investigated using flow visualization and digital particle image velocimetry (DPIV).[5]

DPIV measures the two-dimensional displacement-vector field of particles that are suspended in the flow and illuminated by a thin, pulsed sheet of laser light. Using a CCD camera (480×768 pixels, 30 Hz frame rate), a correlation-window size of 32×32 pixels, and a moving-average step size of 8×8 pixels, the processing results in a field measurement of 96×60 velocity vectors with a temporal resolution of 15 velocity fields per second. With a typical field of view of 11×8 cm, the spatial resolution is 0.23×0.25 cm and the uncertainty in the velocity and vorticity measurement is ±1% and ±3%, respectively.

The sequence of images in Fig. 2 shows the important stages of the laminar/turbulent transition of the vortex ring. The images are front views (along the negative x axis) using dye flow visualization. As Fig. 2-I shows, during the generation and up to $t\approx1.3$ s, the vortex ring remains laminar, After $t\approx1.3$ s, azimuthal bending instabilities similar to those observed by Krutzsch[6,7] and Widnall *et al.*[8] start to develop and mark the beginning of the transition stage. In Figs. 2-II and 2-III, the bending instability leads to a strong and symmetric growth of the ring deformation within $\Delta t\approx0.3$ s. As Fig. 2-IV shows, the latter causes a sudden breakup of the vortex ring at $t\approx2.5$ s which marks the beginning of the turbulent stage. Similar to the photographs published in Refs. 2–4, the side view (along the negative z axis) in Fig. 3 indicates that the turbulent stage is characterized by a strong shedding process of dye into the wake of the vortex ring. Using the initial conditions and the resulting core diameter (see below), the wave numbers predicted by the theoretical models of Widnall *et al.* ($n=7$) and Saffman[9] ($n=8$) are in good agreement with the observed value of $n=8$.

Figure 4 shows results of DPIV measurements in the

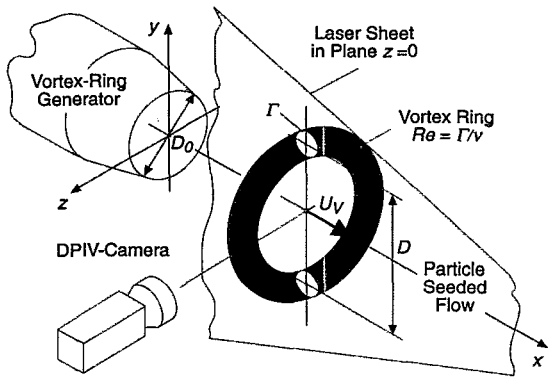

FIG. 1. Schematic of the experimental setup.

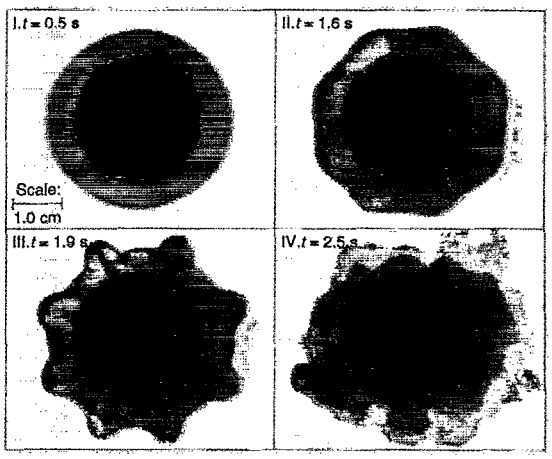

FIG. 2. Front view of the transition of a vortex ring (Re=7500).

 1070-6631/94/6(12)/3806/3/$6.00

FIG. 3. Side view of the turbulent stage (Re=7500).

plane $z=0$ regarding the temporal evolution of the vorticity field (a) and the vortex-ring circulation (b). The circulation was computed from the line integral of the velocity data along the vorticity contour $\omega_z=\pm 2.5\ s^{-1}$ that separates the upper- and lower-core regions from the ambient flow field.

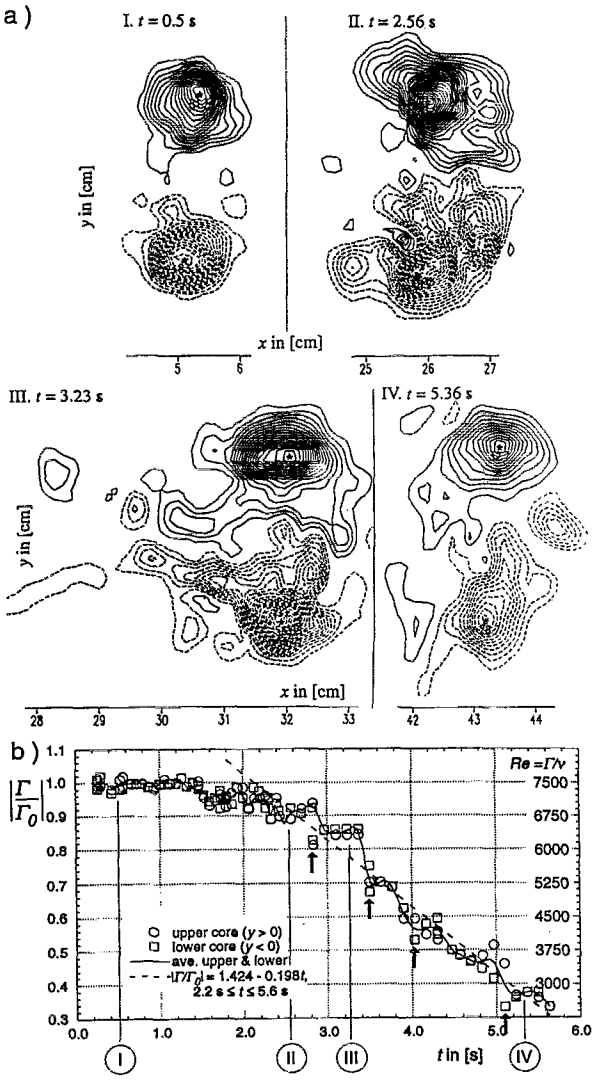

FIG. 4. Temporal evolution of the vorticity field and circulation (Re=7500), (a) ω_z vorticity contours in the plane $z=0$; (b) magnitude of the upper- and lower-core circulation.

During the initial stage, the nearly circular shape and dense distribution of vorticity contours in Fig. 4(a)-I indicate the laminar and highly concentrated core structure of the vortex ring with peak-vorticity values of $|\omega_z|_{max}\approx 80\ s^{-1}$. Up to $t\approx 1.5$ s, the circulation is approximately constant and equal to the initial value of $\Gamma_0=75\ cm^2/s$, i.e., $\Gamma/\Gamma_0\approx 1$. As Fig. 4(a)-II shows, during and shortly after the transition stage between 1.6 s$<t<$2.5 s, the upper and lower cores are symmetrically deformed and show first signs of the turbulent breakup. The latter is indicated by the formation of small and concentrated vorticity regions in the periphery of the core regions. At $t\approx 3.2$ s, Fig. 4(a)-III shows that the on-going breakup leads to the shedding of vortical structures into the wake of the vortex ring. Depending on where the wake structures are cut by the measurement plane, they appear as circular or longitudinal vorticity regions. The longitudinal regions correspond to the elongated dye loops visible in Fig. 3 and, as suggested in Refs. 1 and 4, indicate the presence of axial vorticity (parallel to the plane $z=0$) in the wake. Figure 4(a)-III also shows that, even though the vortex ring is in the turbulent stage, the vorticity distribution in the core region remains concentrated.

As is evident in Fig. 4(b), the vortex-ring circulation does not decrease monotonically, but rather in a staircase-like fashion with periods of nearly constant levels of circulation. This is a remarkable indication of the shedding of vortical structures that contain a finite amount of circulation. The agreement in the evolution of the upper- and lower-core circulation suggests that the shedding occurs symmetrically. Detailed analysis of the vorticity fields indicates that part of the shed structures can be reentrained again into the major core region. This effect is visible in Fig. 4(b) and leads to a small increase of the circulation after the beginning of a shedding cycle (marked by an arrow). Between 2.2 s$\leqslant t\leqslant$5.6 s, the overall decrease of the circulation can be approximated by a linear function of time. It is interesting to note that the decay law $\Gamma\sim t^{-1/2}$ predicted by Glezer and Coles[4] for the total circulation of the ring and wake does not necessarily apply for the vortex ring itself.

After losing 65% of the initial circulation, Fig. 4(a)-IV shows that the vorticity distribution in the core regions is still concentrated and close to circular shape. The loss of circulation to the wake results in a reduction of the Reynolds number of the vortex ring. In the case presented here, it decreases from the initial value of Re=7500 to Re$\approx$2300 at $t=5.6$ s. Therefore, the successive shedding of vorticity leads to the relaminarization of the turbulent vortex ring which is also apparent by the lack of peripheral structures in Fig. 4(a)-IV. In agreement with the visual results of Maxworthy[3] and Vladimirov and Tarasov,[10] the persistence of the regularly structured core regions suggests that only the peripheral regions of the vortex ring are affected by the shedding process, while the local flow in the center of the cores remains stable. As the vorticity fields indicate, the distance between the peak vorticities (i.e., the diameter of the vortex ring) remains approximately constant with $D\approx 2.8$ cm or $D^*=D/D_0\approx 1.4$. A rough estimate of the core size can be obtained from the area that is enclosed by the lowest vorticity contour ($\omega_z=5\ s^{-1}$) at $t=0.5$ s resulting in an initial core diameter of $\sigma\approx 0.5D$.

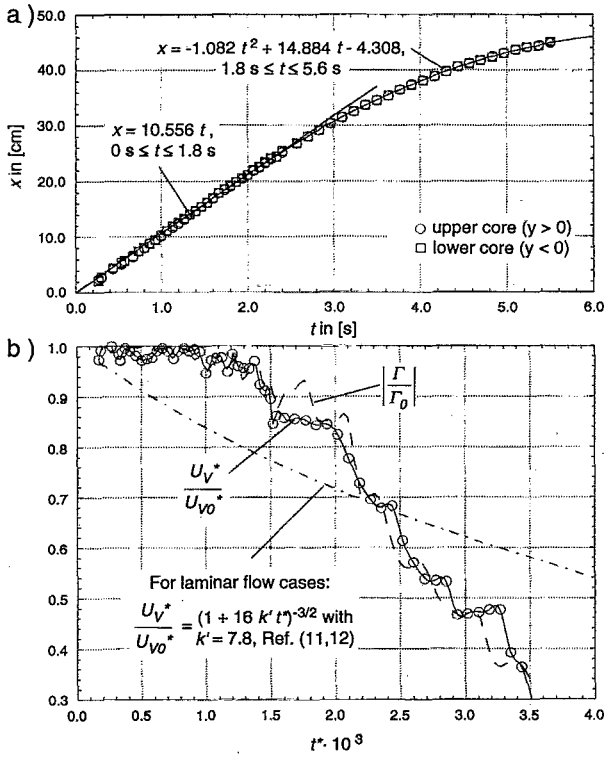

FIG. 5. (a) Trajectory and (b) circulation and propagation speed (Re=7500) in comparison to propagation speed of laminar vortex rings.

In addition to the circulation, the temporal evolution of the trajectory of the vortex ring was measured using the DPIV data. Figure 5(a) shows the downstream distance of the vorticity peaks as a function of time. A Galilean transformation of the instantaneous velocity fields was employed to recover the propagation speed directly from the measured DPIV data. Figure 5(b) shows the obtained result in comparison to the propagation speed of laminar vortex rings ($830 \leqslant \mathrm{Re} \leqslant 1650$).[11,12] According to Ref. 12, the decay of the propagation speed in the laminar flow cases is dominated by viscous diffusion and well described by Saffman's[13] analytical model for thick-cored vortex rings. The latter yields $U_V^* = 16\pi/k(1+16k't^*)^{-3/2}$, where k and k' are experimental constants with $k=14.4$ and $k'=7.8$. Time and propagation speed are normalized by the viscous time scale and the initial conditions, i.e., $t^* = 0.25\nu t/D_0^2$ and $U_V^* = 2\pi U_V D_0/\Gamma_0$. For the comparison in Fig. 5(b), the propagation speeds are normalized by the initial value U_{V0}^* at time $t \approx 0$ s, where U_{V0}^* is equal to 3.49 in the laminar case and 1.77 in the turbulent case.

As the trajectory and velocity measurements indicate, the average decay of the propagation speed in the turbulent stage is a linear function of time and, therefore, much faster than that of laminar vortex rings. It is evident from Fig. 5(b) that the shedding process has a direct impact on the propagation speed. In comparison to the decay of the circulation, the propagation speed decreases approximately with the same periodicity and relative rate per shedding cycle suggesting that $U_V \propto \Gamma$. However, a small and temporally increasing phase shift of $\Delta t \sim 10^{-1}$ s is observed. One might speculate that the time or, equivalently, Reynolds-number-dependent phase shift is a result of the adjustment of the flow field to distortions caused by the shedding process (e.g., interaction of the shed structures with the primary ring and redistribution of vorticity in the core regions).

The circulation data, the propagation speed, and the geometrical spacing of the shed structures visible in Fig. 3 indicate that the shedding frequency decreases weakly over time from $f \approx 2.5$ Hz (St$\approx$0.5) to $f \approx 1.5$ Hz (St$\approx$0.3). The Strouhal number is based on the initial conditions $D_0=2$ cm and $U_{V0} \approx 10$ cm/s and defined by $\mathrm{St} = fD_0/U_{V0} = (D_0/\Delta s)(U_V/U_{V0})$. In agreement with the frequency and propagation speed measurements, the visual spacing is approximately constant ($\Delta s/D_0 \approx 1.3$) yielding a constant, local Strouhal number of $\mathrm{St} = fD/U_V = D/\Delta s = 1 \pm 0.1$. This value is approximately 50% lower than the local Strouhal numbers that were obtained from acoustic radiation data[14] and visual measurements[15] of the shedding frequency of high Reynolds number turbulent vortex rings ($\mathrm{Re} \sim 10^4$ to 10^5).

In conclusion, the present results indicate that the wake of a turbulent vortex ring consists of vortical structures that are shed from the peripheral regions of the ring. This shedding process leads to a nonmonotonic and staircase-like decay of the circulation and the propagation speed of the vortex ring. The flow in the core regions remains stable, while the decay of the circulation results in the reduction of the Reynolds number and the relaminarization of the vortex ring.

ACKNOWLEDGMENTS

This work has been supported by the Office of Naval Research (ONR–URI Grant No. N00014-92-J-1610) under the program management of Dr. Edwin Rood.

[1] K. Shariff and A. Leonard, "Vortex rings," Annu. Rev. Fluid Mech. **24**, 235 (1992).
[2] D. W. Sallet and R. S. Widmayer, "An experimental investigation of laminar and turbulent vortex rings in air," Z. Flugwiss. **22**, 207 (1974).
[3] T. Maxworthy, "Turbulent vortex rings," J. Fluid Mech. **64**, 227 (1974).
[4] A. Glezer and D. Coles, "An experimental study of a turbulent vortex ring," J. Fluid Mech. **211**, 243 (1990).
[5] C. E. Willert and M. Gharib, "Digital particle image velocimetry," Exp. Fluids **10**, 181 (1991).
[6] C. H. Krutzsch, "Über ein instabiles Gebiet bei Wirbelringen," Z. Angew. Math. Mech. **16**, 352 (1936).
[7] C. H. Krutzsch, "Über eine experimentell beobachtete Erscheinung an Wirbelringen bei ihrer translatorischen Bewegung in wirklichen Flüsigkeiten," Ann. Phys. **35**, 497 (1939).
[8] S. E. Widnall, D. B. Bliss, and C. Y. Tsai, "The instability of short waves on a vortex ring," J. Fluid Mech. **66**, 35 (1974).
[9] P. G. Saffman, "The number of waves on unstable vortex rings," J. Fluid Mech. **84**, 625 (1978).
[10] V. A. Vladimirov and V. F. Tarasov, "Structure of turbulence near the core of a vortex ring," Sov. Phys. Dokl. **24**, 254 (1979).
[11] A. Weigand, "The response of a vortex ring to a transient, spatial cut," Ph.D. thesis, Department of Applied Mechanics and Engineering Sciences, University of California, San Diego, 1993.
[12] A. Weigand and M. Gharib, "Some experimental results on laminar vortex rings," submitted to Phys. Fluids (1994).
[13] P. G. Saffman, "The velocity of viscous vortex rings," Stud. Appl. Math. **49**, 371 (1970).
[14] M. Yu. Zaitsev, V. F. Kop'ev, A. G. Munin, and A. A. Potokin, "Sound radiation by a turbulent vortex ring," Sov. Phys. Dokl. **35**, 488 (1990).
[15] D. Auerbach, "Stirring properties of vortex rings," Phys. Fluids A **3**, 1351 (1991).